Title

Isosteres of hydroxypyridinethione as drug-like pharmacophores for metalloenzyme inhibition

Journal

JBIC Journal of Biological Inorganic Chemistry, 23(7)

ISSN

0949-8257

Authors

Adamek, Rebecca N
Credille, Cy V
Dick, Benjamin L
et al.

Publication Date

2018-10-01

DOI

10.1007/s00775-018-1593-1

Peer reviewed

HHS Public Access

Author manuscript

J Biol Inorg Chem. Author manuscript; available in PMC 2019 October 01.

Published in final edited form as:

J Biol Inorg Chem. 2018 October ; 23(7): 1129–1138. doi:10.1007/s00775-018-1593-1.

Isosteres of Hydroxypyridinethione as Druglike Pharmacophores for Metalloenzyme Inhibition

Rebecca N. Adamek, **Cy V. Credille**, **Benjamin L. Dick**, and **Seth M. Cohen**✉

Department of Chemistry and Biochemistry, University of California, San Diego, La Jolla, CA 92093

Abstract

Hydroxypyridine thiones (HOPTOs) are strong ligands for metal ions and are therefore potentially useful pharmacophores for inhibiting metalloenzymes relevant to human disease. However, HOPTOs have been sparingly used in drug discovery efforts due, in part, to concerns that this scaffold will act as promiscuous non-selective metalloenzyme inhibitor, as well as poor pharmacokinetics (PK), which may undermine drug candidates containing this functional group. In order to advance HOPTOs as a useful pharmacophore for metalloenzyme inhibitors, a library of 22 HOPTO isostere compounds has been synthesized and investigated. This library demonstrates that it is possible to maintain the core metal-binding pharmacophore (MBP) while generating diversity in structure, electronics, and PK properties. This HOPTO library has been screened against a set of four different metalloenzymes, demonstrating that while the same metal-binding donor atoms are maintained, there is a wide range of activity between metalloenzyme targets. Overall, this work shows that HOPTO isosteres are useful MBPs and valuable scaffolds for metalloenzyme inhibitors.

Keywords

Fragment-based Drug Discovery; Hydroxypyridinethione; Inhibitor; Isostere; Metal-binding Pharmacophore; Metalloenzyme

INTRODUCTION

Metalloenzymes constitute at least one-third of all enzymes, are involved in a broad range of in vivo functions, and represent a validated class of clinical targets.[1-3] Metalloenzymes have been linked to a number of human diseases including cancer and heart disease,[4] and have been implicated as targets in both pathogenic bacterial[5] and viral vectors.[6] Small molecule therapeutics containing metal-binding pharmacophores (MBPs) designed to coordinate the active site metal ion offer an appealing approach in treating diseases linked to metalloenzymes.[7]

Hydroxypyridinethiones (HOPTOs) are natural products derived from the *Allium stipitatum* or drumstick onion plant,[8] and are a chemical scaffold highly suited for metal binding.

✉ scohen@ucsd.edu.

There are three isomeric HOPTO scaffolds, with each bearing a thione and hydroxyl donor atom metal coordination motif, as shown in Figure 1. These ligands are well established in the field of inorganic chemistry and are known to form stable, 5-member coordination rings with a variety of metal ions.[9] This strong metal binding combined with the heterocyclic nature of the HOPTO scaffold imparts a high binding affinity for metalloenzymes, implying that HOPTOs can be a useful warhead for drug discovery campaigns against metalloenzymes.

However, despite their strong affinity for metal ions and metalloenzymes, the therapeutic potential of the HOPTO MBP has been underexploited. Only zinc pyrithione (a.k.a., 1,2-HOPTO = 1-hydroxypyridine-2(1*H*)-thione) (Figure 1) is widely used for its anti-microbial properties[10] as the active ingredient of anti-dandruff shampoos[11] and in anti-fouling agents for paints.[12] There are no reports of FDA approved drugs containing the HOPTO scaffold for human internal use. This is in contrast to the analogous hydroxy-pyridinone (HOPO) MBP, derivatives of which have been used in applications, ranging from food additives to pharmaceuticals.[13] In particular, HOPO derivatives have been used as MBPs in metalloenzyme inhibitors, such as the FDA-approved HIV integrase inhibitors raltegravir[14] (Figure 1), and dolutegravir,[15] in addition to being utilized as a MBP warhead in innumerable metalloenzyme inhibitor campaigns. Considering that HOPTOs and HOPOs only differ by a thione versus ketone respectively, it is surprising that the HOPTO scaffold has not enjoyed the same therapeutic utility as the HOPO scaffold.

In large part, the lack of use of the HOPTO scaffold can be attributed to a broader general concern around metalloenzyme inhibitors, of which those containing thiols are viewed with particular reservation (despite the clinical success of compounds such as Captopril).[16-18] Metalloenzyme inhibitors have suffered under the impression that if a molecule is able to bind metal, it will act indiscriminately and display broad off-target effects by inhibiting all available metalloenzymes.[19] However, studies by Chen[20] and Day[21] demonstrate otherwise, showing that metalloenzyme inhibitors are as selective in binding to their respective targets as other small molecule inhibitors, and are not titrated away by the presence of alternate, off-target metalloenzymes. Furthermore, metalloenzymes are the validated target of multiple drug discovery campaigns, with there being approximately 64 FDA-approved metal-binding metalloenzyme inhibitors,[4,22,23] clearly indicating that the presence of a MBP does not diminish the therapeutic potential of a molecule.

As for the thiol, there has been concern over potential toxicity issues. There have been reports of terminal thiol inhibitors such as L-744,832 against farnesyl transferase, which failed Phase I clinical trials due to off-target effects.[24,25] However, it critical to understand that the thione present in the HOPTO scaffold is not a thiol and therefore has a different physiochemical and PK profile. As the HOPTO thione predominately exists in the sp^2 hybridization with 53:1 thione to thiol,[26] it is not subjected to the same reactivity (and hence toxicity) associated with the thiol moiety. Furthermore, the bidentate metal-binding profile of HOPTOs grants potentially greater metalloenzyme specificity than the monodentate nature of a terminal thiol.

Outside of the stigma associated with MBPs, the only real drawback associated with the HOPTO scaffold has been a relatively poor logP, leading to limited aqueous solubility,[27] as well as a limited scope of meaningful structure activity relationship (SAR) studies on how modifications to the MBP itself affect overall metal-binding and inhibitory activity. Thus, detailed herein is a summary of useful HOPTO isosteres and analogues designed with the purpose of improving PK and maintaining metal binding properties (Figure 2). We have prepared a 22 component HOPTO metal-binding isostere (MBI) library, demonstrating that it is possible to access a wealth of synthetic diversity with electronic and PK tunability while maintaining donor atoms critical for metal binding. In addition to this library, we have also prepared routes to derivatives of select members of this HOPTO library as a means of demonstrating their potential for fragment growth and merging strategies.

Finally, for the purpose of evaluating these novel HOPTO scaffolds as fragments useful to medicinal chemistry, human carbonic anhydrase II (hCAII), matrix metalloprotease-12 (MMP-12), New Delhi Metallo-ß-lactamase-1 (NDM-1), and influenza endonuclease (PA_N) were selected as metalloenzyme targets to test the validity and selectivity of the HOPTO library (Figure 3). hCAII and MMP-12 are both mononuclear Zn^{2+}-dependent human metalloenzymes, where hCAII regulates blood pH and the MMPs have long been established as cancer targets. NDM-1 is a dinuclear Zn^{2+}-dependent metalloenzyme that confers bacterial resistance to ß-lactam antibiotics, and PA_N is a conserved dinuclear Mn^{2+}-dependent metalloenzyme vital for influenza virus replication. PA_N was included as the *O,S* donor is expected to be less suitable for the Mn^{2+} active site (based on hard-soft acid-base theory) when compared to the Zn^{2+}-dependent metalloenzymes studied here.[28,29] HOPTOs **1** – **22** were screened against these four metalloenzymes at 200 μM and demonstrate that taking a metal-centric approach and fine-tuning the SAR of just the core MBP generates different selectivity amongst these metalloenzymes even though the ligand donor set is maintained.

MATERIALS AND METHODS

Materials.

All reactants and reagents were purchased from either Sigma-Aldrich, Alfa-Aesar, or Combi-blocks and used with no additional purification. Synthetic protocols and details for **1** – **37** are reported in the SI. Absorbance assays were performed using a BioTek Synergy HT microplate reader. Fluorescence assays were performed using either a BioTek Synergy HT microplate reader or a BioTek Synergy H4 microplate reader. hCAII was prepared as previously reported,[30] MMP-12 was purchased from Enzo Life Sciences (Farmingdale, NY, USA), NDM-1 was supplied as a gift from Dr. David Tierney (U. Miami, Ohio), and influenza endonuclease was expressed and purified as previously reported.[31]

Pharmacokinetic Properties.

All calculated PK data was determined through ChemAxon. Experimental logP and $logD_{7.4}$ for **1**, **4**, **9**, and **14** was determined using a Sirius T_3 instrument. Both pK_a and logP were performed in 0.15 M KCl with 0.5 M HCl and KOH. First the pK_a was experimentally determined through triplicate potentiometric titrations,[32,33] Sample sizes contained

approximately 0.70 mg of MBI for pK_a measurements. The experiments were titrated from pH 12.0 to 2.0, and standard deviations were determined from fitting the three replicate runs. As **1** had poor aqueous solubility, it was necessary to include HPLC grade MeOH in the sample analysis.

logP was experimentally determined through potentiometric titrations in the presence of differing ratios of octanol and water in triplicate runs.[32,33] Sample sizes contained approximately 0.50 mg of MBI for logP measurements. Again the experiments were titrated from pH 12.0 to 2.0, and standard deviations were determined from fitting the three replicate runs. $LogD_{7.4}$ was then calculated from the measured pK_a and logP values.

MMP-12 Assays.

MMP-12 and OmniMMP fluorogenic substrate were purchased as an assay kit from Enzo Life Sciences, and the assay was performed in a Costar black 96-well plate. Each well contained a total volume of 100 μL including buffer (50 mM HEPES, 10 mM $CaCl_2$, 0.05% Brij-35, pH 7.5), human recombinant MMP-12 (0.7 U per well, Enzo Life Sciences), inhibitor (200 μM), and fluorogenic OmniMMP substrate (4 μM MCA-Pro-Leu-Gly-Leu-DPA-Ala-Arg-NH_2-AcOH, Enzo Life Sciences). The enzyme and inhibitor were initially incubated together for 15 min at 37 °C, after which the reaction was initiated by substrate addition. The change in fluorescence was monitored for 20 min with excitation at 320 nm and reading emission at 400 nm. The negative control wells contained no inhibitor and were arbitrarily set as 100% enzyme activity.

hCAII Assays.

hCAII was prepared as previously reported,[30] and the assay was performed in a Costar clear 96-well plate. Each well contained a total volume of 100 μL including buffer (50 mM HEPES, 100 mM $NaSO_4$, pH 8.0), hCAII (100 nM), inhibitor (200 μM), and *p*-nitrophenyl acetate substrate (500 μM). The enzyme and inhibitor were initially incubated together for 15 min at room temperature, after which the reaction was initiated by substrate addition. The change in absorbance was monitored for 20 min at 405 nm. The negative control wells contained no inhibitor and were arbitrarily set as 100% enzyme activity.

NDM-1 Assays.

NDM-1 was supplied as a gift from David Tierney, and the Fluorocillin Green substrate was purchased from ThermoFisher. The assay was performed in a Costar black 96-well plate. Each well contained a total volume of 100 μL including buffer (50 mM HEPES, 2 mM CHAPS, 5 μM Zn-SO_4, pH 7.0), NDM-1 (100 pM), inhibitor (200 μM), and fluorocillin green substrate (87 nM). The enzyme and inhibitor were initially incubated together for 20 min at room temperature, after which the reaction was initiated by substrate addition. The change in fluorescence was monitored for 20 min with excitation at 485 nm and reading emission at 528 nm. The negative control wells contained no inhibitor and were arbitrarily set as 100% enzyme activity. IC_{50} values were determined by incubating various concentrations of inhibitor with the enzyme using the aforementioned conditions, and the data were fit using the GraphPad Prism software suite.

PA_N Assays.

PA_N was prepared as previously reported,[31] and the fluorescent ssDNA-oligo substrate was purchased from Sigma-Aldrich. The assay was performed in a Costar black 96-well plate. Each well contained a total volume of 100 μL including buffer (20 mM Tris, 150 mM NaCl, 2 mM $MnCl_2$, 2 mM $MgCl_2$, 10 mM ß-mercaptoethanol, 0.2% Triton-X100, pH 8.0), PA_N (25 nM), inhibitor (200 μM), and fluorescent ssDNA-oligo substrate (200 nM). A single-stranded, 17-mer DNA substrate labeled with a 5'-FAM fluorophore and a 3'-TAMRA quencher ([6-FAM]AATCGCAGGCAGCACTC[TAM]) was synthesized by Sigma-Aldrich and was used to measure PA_N cleavage. There was no pre-incubation period, and the reaction was initiated by substrate addition. The change in fluorescence was monitored for 45 min at 37 °C with excitation at 485 nm and reading emission at 528 nm. The negative control wells contained no inhibitor and were arbitrarily set as 100% enzyme activity.

RESULTS AND DISCUSSION

Library Development.

The HOPTO library was synthesized as detailed in the SI. Particular focus was placed on the inclusion of heteroatoms as a means of fine-tuning the HOPTO ring electronics, as seen in **14**, as well as the use of bicyclic systems to introduce more lipophilicity and directionality (Figure 2). In particular, **6 – 8** can be considered as 'napthyl' isosteres of 1,2-HOPTO and as a group are designed to evaluate the effect of moving the steric bulk of an additional phenyl ring around the 1,2-HOPTO core. Likewise, **15** and **16** are also bicyclic analogues of 2,3-HOPTO, and **18** presents the bicyclic version of 3,4-HOPTO. Compound **9** is a deazapurine analogue of 1,2-HOPTO that was designed to have improved water solubility; however, as **9** has a potential alternate metal binding site, **10** and **11** were prepared as probes of this secondary metal-binding functionality. Furthermore, as **2**, **4**, and **5** are also designed to contain a secondary metal-binding site, **3** was included as a control for this second metal-binding site. Finally **20** and **21** are included as analogues of the HOPTO scaffold itself with no heteroatom and an oxygen heteroatom, respectively.

Elaborated HOPTO Derivatives.

Derivatives of select HOPTO isosteres were prepared as described in the Supporting Information. Compounds **2**, **4**, **6**, **9**, and **19** were selected as representative scaffolds for derivatization as the fragment growth protocols applied to these molecules are easily extrapolated to other members of the HOPTO library. Derivatization focused on fragment growth methods commonly seen in fragment-based drug discovery (FBDD) strategies, with a particular emphasis was placed on techniques such as metal catalyzed cross couplings (**23 – 26**, **30 – 34**), sulfonamide couplings (**27 – 29**), as well as nucleophilic substitution (**35 – 37**). The ability to elaborate these HOPTO isosteres through such varied synthetic methodologies demonstrates that this library is more than just novel MBP fragments, but contains structures that readily have the capacity to be developed into lead molecules. Routes to prepare such derivatives will facilitate future medicinal chemistry efforts based on these HOPTO scaffolds.

Pharmacokinetics.

In terms of assessing the druglike potential of a molecule, Lipinski's Rule-of-Five has long been the standard guideline for determining oral bioavailability,[34] along with addendums by Veber[35] and Clark.[36] Briefly, some of the more pertinent values include ClogP as a measure of lipophilicity, ClogD a pH sensitive measure of lipophilicity that takes into account ionization states, ClogS accounts for aqueous solubility (note that ClogD and ClogS are typically reported at or near physiological pH 7.4), rotatable bonds affect molecular flexibility, and (topological) polar surface (PSA or TPSA) area impacts the potential for membrane permeability. [34-36] As fragments typically have overall less molecular weight than fully elaborated lead molecules, it has been suggested that fragments require a more scaled-down approach than the Rule-of-Five, and that a "Rule-of-Three" is more amenable in assessing fragment-based leads for drug discovery.[37] A summary of the idealized values of these PK constraints for both fragments and elaborated leads is shown in Table 1, with a comparison of how they apply to each member of the HOPTO library. In particular, PSA, ClogP, ClogD, and ClogS were chosen as the primary criteria to evaluate the druglikeness of the HOPTO library as the other considerations of molecular weight, number of hydrogen bond donors and acceptors, and rotatable bonds are readily met.

Pharmacokinetic (PK) values were calculated using available software from ChemAxon, following the precedent by Lassalas et al.[38] Briefly, the PSA ranges from 55.56 to 110.11 $Å^2$, with ClogP ranging from −0.52 to 2.54, $CLogD_{7.0}$ from −2.44 to 2.41, and $ClogS_{7.0}$ from −3.72 to 0.03, so that there is a 3 – 5 log difference between the calculated log values (Table 1). It is worth noting that these calculated values are well within the acceptable parameters for the Rule-of-Three. Moreover, the fact that these compounds cover a 3 – 5 log range is highly encouraging from a drug discovery perspective, as this breadth of values is indicative of tunability in terms of PK properties, a necessary feature for drug development. In terms of the PSA, the library is well tolerated by the Rule-of-Five, but is technically slightly high by the Rule-of-Three for fragments. This polarity is a necessary feature for metal binding as Lewis bases are required to engage in meaningful interactions with metal cations. The higher PSA is not particularly concerning, as a general profile to avoid drug toxicity is a PSA greater than 75 $Å^2$ coupled with a logP less than 3,[39] which are values well matched by the HOPTO MBIs.

In order to corroborate the calculated PK values with actual experimental data, the logP and $logD_{7.4}$ were experimentally determined for **1**, **4**, **9**, and **14** as representative compounds. For **1** the logP = 0.51±0.01 and $logD_{7.4}$ = −1.86; for **4** the logP = 0.49±0.02 and $logD_{7.4}$ = −1.78; for **9** the logP = 0.37±0.03 and $logD_{7.4}$ = −2.00; and for **14** the logP = −1.02±0.18 and $logD_{7.4}$ = ÷1.15. The measured $logD_{7.4}$ values are not identical to the predicted calculated values; however, this is not atypical as cyclic, acidic moieties have been previously reported to have similar discrepancies between computational and experimental logD values.[38] Furthermore, the experimentally determined $logD_{7.4}$ for **1**, **4**, **9,** and **14** were much lower than the $ClogD_{7.0}$, indicating that these HOPTOs are likely to be more water soluble than predicted; a property that bodes well for the druglikeness of these HOPTO based compounds. In short, the HOPTO library is tolerated by the canonical Rule-of-Three

used to evaluate fragments for lead development, which is an excellent indicator for the potential of the HOPTO scaffold as a lead in inhibitor development against metalloenzymes.

Model Complexes.

Zinc hydrotris(3,5-phenylmethylpyrazolyl)borate [($Tp^{Ph,Me}$)Zn(MBI)] complexes were prepared of **4**, **9**, and **14**; these complexes were crystallized and their structure determined by single-crystal X-ray diffraction (Figure 4). These compounds were selected as representative models of the HOPTO library and all demonstrate that the typical HOPTO binding motif (as exemplified by 1,2-HOPTO, Figure 1) is conserved even after significant electronic and structural changes have been introduced to the HOPTO ring. These complexes maintain the binding pose of equatorial thione and axial oxygen with no perturbations to the surrounding ligand environment of the TP complex. This HOPTO binding is consistent with the 1,2-HOPTO, 2,3-HOPTO, and 3,4-HOPTO previously reported.[9,40] The only discernable difference is that the ligands show different canted angles where the HOPTO ligand is tilted further forward or back compared to 1,2-HOPTO, but this effect could very well be artifacts of crystal packing. These [($Tp^{Ph,Me}$)Zn(MBI)] model complexes demonstrate that the HOPTO isosteres maintain the same metal binding mode as the parent HOPTO scaffolds, regardless of how the electronics and substituents are modified.

Metalloenzyme Assays.

The activity of each metalloenzyme was monitored via kinetic assays that measured either an increase in fluorescence or absorbance upon substrate hydrolysis (see Experimental section for details). All compounds were incubated with each metalloenzyme at a fragment concentration of 200 μM, with the percent inhibition of each fragment displayed in Table 2. The results of these activity screens shows widely varying SAR preferences for each individual metalloenzyme, even though the same core ligand donor atoms are maintained across all of the MBIs.

Both MMP-12 and hCAII have similar active sites that rely on a tris(histidine) coordinated Zn^{2+} ion for catalytic activity, yet hCAII displays far fewer hits with only **6** having relevant inhibition against hCAII (Table 2), whereas **4**, **5**, **6**, **11**, and **17** all display 94% or better inhibition against MMP-12. A likely reason for the selectivity observed in hCAII, as previously detailed in work by Martin,[41] is that the protein active site environment can impart a great deal of control on what ligands are able to effectively access the Zn^{2+} ion within the active site. The hCAII active site is fairly sterically and electrostatically constricted with both hydrophobic and hydrophilic regions, and therefore only allows a select number of ligands to bind efficiently. Conversely, the active site of MMP-12 is relatively more open and therefore allows more ligands to bind.

While most reported metallo-ß-lactamases (MBLs) all have similar active site coordination geometry, NDM-1 was selected as a representative MBL as it is the most prevalently occurring worldwide,[42] and is currently an important target due to its relevance in causing antibiotic resistance.[43] The NDM-1 active site is dinuclear Zn^{2+} with Zn_1 coordinated by a tris-His group in tetrahedral geometry, and Zn_2 coordinated by Cys, Asp, and His in a distorted tetrahedral geometry.[44] A catalytic water sits coordinated mu between the two

Zn^{2+} ions, and is used as the nucleophile to hydrolyze ß-lactam bonds during NDM-1 activity.[44] During inhibition assays, as the Zn_2 site is relatively less tightly bound with a K_d value of 2 μM,[45] excess Zn^{2+} was supplied at a concentration of 5 μM to ensure the Zn_2 site was fully occupied. In addition, the presence of excess metal in the assay buffer prevents metal stripping by the HOPTO ligands, which may be an issue at the relatively high concentrations of fragment utilized in these early screens. While it is possible to make the argument that including excess Zn^{2+} in the assay buffer would only result in titrating away the ligand due to formation of the $Zn(HOPTO)_2$ complex, this is not a concern as this homoleptic complex would still be able to dissociate and allow for ligand binding at the enzyme active site to occur. In turn, such event would indicate that the HOPTO ligand has a preference for the metal in the active site over the free metal in solution, again highlighting the selectivity dictated by active site environment argument.

From the inhibitor screen at 200 μM, **4**, **5**, **6**, **9**, **11**, **17**, and **21** all performed well against NDM-1, with greater than 90% inhibition. All of the compounds that may have additional donor atoms (**2**, **4**, **5**, and **9**) for binding both metal centers were among the most active NDM-1 inhibitors. It is possible that these compounds are binding both of the active site Zn^{2+} ions, thereby generating increased inhibitory activity. Without structural data, it is difficult to predict if both of the Zn^{2+} ions are coordinated by these HOPTO ligands, but it is reasonable to assume that these ligands are bound to one metal ion and likely bridging between the two Zn^{2+} ions. IC_{50} values for **4**, **5**, **6**, and **9** were determined to be 35, 100, 40, and 43, μM respectively (see SI for experimental data). It is encouraging that many members of the HOPTO library performed this well against NDM-1, even when challenged with excess Zn^{2+}, indicating that these HOPTO fragments have great potential to be used in inhibitor discovery campaigns against MBLs such as NDM-1. In particular, **9** stands out as a lead fragment for further development as it was the most selective for NDM-1 over MMP-12 and hCAII.

PA_N was used as a compliment to NDM-1 as it is also a dinuclear metalloenzyme but relies on active site Mn^{2+} for catalysis, providing a control for a hard Lewis acid metal in comparison to the softer Zn^{2+}. The PA_N active site consists of Mn_1 bound by Glu, Asp, and four waters in an octahedral geometry, and Mn_2 bound by His, Asp, Glu, two waters, and the carbonyl backbone of an Ile in a distorted octahedral geometry (Figure 3).[46] As the Mn_1 is relatively more labile, the influenza endonuclease assay also contained excess Mn^{2+} (and Mg^{2+}), to be consistent with previous reports of PA_N activity assays and for similar reasons as described in the NDM-1 assay.[31] However, the effect of excess Mn^{2+} metal ions on the overall activity of metal binding inhibitors has been found to be insignificant so long as the total concentration of metal ions is above the K_d of the more labile metal binding site.[47] Overall **5**, **7**, **21**, and **22** had the best activity against endonuclease with greater than 90% inhibition. It is expected that fewer compounds emerged as hits against PA_N than NDM-1 due to hard-soft Lewis acid base theory. Furthermore, it is also interesting to note that the two napthyl HOPTO isosteres, **6** and **7**, showed widely varying activity that was contrary to that observed with the other three metalloenzymes studied here.

Finally, it is worth noting that control compound **20** showed little to no activity against any of the metalloenzymes tested. As **20** still has the same *O,S* donor atoms and therefore the

same binding motif, the lack of activity in **20** is indicative of the importance of the nitrogen heteroatom in the HOPTO MBP. As stated previously, the nitrogen heteroatom promotes the thione hybridization, so that the HOPTO ligand exists as a monoanionic species, thereby facilitating metal binding under physiological conditions. In short, the HOPTO scaffold is well suited and useful pharmacophore for designing inhibitors against metalloenzymes.

CONCLUDING REMARKS

This library of HOPTO isosteres demonstrate that the HOPTO scaffold is electronically tunable, and can access a wide range of PK properties without sacrificing metal-binding capacity. Moreover, these HOPTO fragments display strong inhibition activity, and despite containing the same ligand donor atoms, they have remarkable selectivity between different metalloenzymes. These results once again highlight the validity of a metal-centric approach and demonstrate, even at the fragment level, small modifications to the SAR of the MBP can have drastic effects on metalloenzyme inhibition. In all, this work should help to expand the utility of metal binding inhibitor scaffolds such as HOPTOs and eventually lead to new avenues of therapeutics against metalloenzymes.

Supplementary Material

Refer to Web version on PubMed Central for supplementary material.

ACKNOWLEDGEMENTS

This work was supported by the National Institutes of General Medical Sciences (R01-GM111926). R.N.A. was supported by the National Institute of Health Chemical Biology Interfaces Training Grant UC San Diego (T32GM112584-01). We thank Prof. Arnold Rheingold and Dr. Curtis Moore (U.C. San Diego) for assistance with crystallographic data collection and structure determination. We also thank Dr. Yongxuan Su (U.C. San Diego) for mass spectrometry sample analysis at The Molecular Mass Spectrometry Facility. We thank Dr. Carlo Ballatore for aid with Sirius PK analysis. We thank Dr. Yuyong Ma for preparing compound **11**. S.M.C. is a co-founder, has an equity interest, and receives income as member of the Scientific Advisory Board for Cleave Biosciences and is a co-founder, has an equity interest, and a member of the Scientific Advisory Board for Forge Therapeutics. Both companies may potentially benefit from the research results of certain projects in the laboratory of S.M.C. The terms of this arrangement have been reviewed and approved by the University of California, San Diego in accordance with its conflict of interest policies.

NONSTANDARD ABBREVIATIONS

hydroxypyridine
(HOPO)

hydroxypyridinethione
(HOPTO)

metal-binding isostere
(MBI)

metal-binding pharmacophore
(MBP)

pharmacokinetic

(PK)

References

(1). Holm RH; Kennepohl P; Solomon EI Structural and Functional Aspects of Metal Sites in Biology. Chem. Rev 1996, 96, 2239–2314. [PubMed: 11848828]

(2). Andreini C; Bertini I; Cavallaro G; Holliday GL; Thornton JM Metal Ions in Biological Catalysis: from Enzyme Databases to General Principles. J. Biol. Inorg. Chem 2008, 13, 1205–1218. [PubMed: 18604568]

(3). Waldron KJ; Rutherford JC; Ford D; Robinson NJ Metalloproteins and Metal Sensing. Nature 2009, 460, 823–830. [PubMed: 19675642]

(4). Yang Y; Hu XQ; Li QS; Zhang XX; Ruan BF; Xu J; Liao CZ Metalloprotein Inhibitors for the Treatment of Human Diseases. Curr. Top. Med. Chem 2016, 16, 384–396. [PubMed: 26268345]

(5). Moellering RC NDM-1 - A Cause for Worldwide Concern. New Engl. J. Med 2010, 363, 2377–2379. [PubMed: 21158655]

(6). Ju H; Zhang J; Huang BS; Kang DW; Huang B; Liu XY; Zhan P Inhibitors of Influenza Virus Polymerase Acidic (PA) Endonuclease: Contemporary Developments and Perspectives. J. Med. Chem 2017, 60, 3533–3551. [PubMed: 28118010]

(7). Agrawal A; Johnson SL; Jacobsen JA; Miller MT; Chen LH; Pellecchia M; Cohen SM Chelator Fragment Libraries for Targeting Metalloproteinases. Chemmedchem 2010, 5, 195–199. [PubMed: 20058293]

(8). Kubec R; Krejcova P; Simek P; Vaclavik L; Hajslova J; Schraml J Precursors and Formation of Pyrithione and Other Pyridyl-Containing Sulfur Compounds in Drumstick Onion, Allium stipitatum. J. Agr. Food Chem 2011, 59, 5763–5770. [PubMed: 21510712]

(9). Puerta DT; Lewis JA; Cohen SM New Beginnings for Matrix Metalloproteinase Inhibitors: Identification of High-Affinity Zinc-Binding Groups. J. Am. Chem. Soc 2004, 126, 8388–8389. [PubMed: 15237990]

(10). Dinning AJ; Al-Adham ISI; Eastwood IM; Austin P; Collier PJ Pyrithione Biocides as Inhibitors of Bacterial ATP Synthesis. J. Appl. Microbiol 1998, 85, 141–146. [PubMed: 9721664]

(11). Schwartz JR Zinc Pyrithione: A Topical Antimicrobial With Complex Pharmaceutics. J. Drugs Dermatol 2016, 15, 140–144. [PubMed: 26885780]

(12). Konstantinou IK; Albanis TA Worldwide Occurrence and Effects of Antifouling Paint Booster Biocides in the Aquatic Environment: A Review. Environ. Int 2004, 30, 235–248. [PubMed: 14749112]

(13). Jakupec MA; Galanski M; Arion VB; Hartinger CG; Keppler BK Antitumour Metal Compounds: more than Theme and Variations. Dalton Trans. 2008, 183–194. [PubMed: 18097483]

(14). Summa V; Petrocchi A; Bonelli F; Crescenzi B; Donghi M; Ferrara M; Fiore F; Gardelli C; Paz OG; Hazuda DJ; Jones P; Kinzel O; Laufer R; Monteagudo E; Muraglia E; Nizi E; Orvieto F; Pace P; Pescatore G; Scarpelli R; Stillmock K; Witmer MV; Rowley M Discovery of Raltegravir, a Potent, Selective Orally Bioavailable HIV-Integrase Inhibitor for the Treatment of HIV-AIDS Infection. J. Med. Chem 2008, 51, 5843–5855. [PubMed: 18763751]

(15). Gunthard HF; Saag MS; Benson CA; del Rio C; Eron JJ; Gallant JE; Hoy JF; Mugavero MJ; Sax PE; Thompson MA; Gandhi RT; Landovitz RJ; Smith DM; Jacobsen DM; Volberding PA Antiretroviral Drugs for Treatment and Prevention of HIV Infection in Adults 2016 Recommendations of the International Antiviral Society-USA Panel. Jama-J. Am. Med. Assoc 2016, 316, 191–210.

(16). Cushman DW; Ondetti MA Design of Angiotensin Converting Enzyme Inhibitors. Nat. Med 1999, 5, 1110–1112. [PubMed: 10502801]

(17). Pfeffer MA; Braunwald E; Moye LA; Basta L; Brown EJ; Cuddy TE; Davis BR; Geltman EM; Goldman S; Flaker GC; Klein M; Lamas GA; Packer M; Rouleau J; Rouleau JL; Rutherford J; Wertheimer JH; Hawkins CM Effect of Captopril on Mortality and Morbidity in Patients with Left-Ventricular Dysfunction after Myocardial-Infarction - Results of the Survival and Ventricular Enlargement Trial. New Engl. J. Med 1992, 327, 669–677. [PubMed: 1386652]

(18). Lewis EJ; Hunsicker LG; Bain RP; Rohde RD The Effect of Angiotensin-Converting Enzyme-Inhibition on Diabetic Nephropathy. New Engl. J. Med 1993, 329, 1456–1462. [PubMed: 8413456]

(19). Baell J; Walters MA Chemistry: Chemical Con Artists Foil Drug Discovery. Nature 2014, 513, 481–483. [PubMed: 25254460]

(20). Chen Y; Cohen SM Investigating the Selectivity of Metalloenzyme Inhibitors in the Presence of Competing Metalloproteins. Chemmedchem 2015, 10, 1733–1738. [PubMed: 26412596]

(21). Day JA; Cohen SM Investigating the Selectivity of Metalloenzyme Inhibitors. J. Med. Chem 2013, 56, 7997–8007. [PubMed: 24074025]

(22). Kinch MS; Haynesworth A; Kinch SL; Hoyer D An Overview of FDA-Approved New Molecular Entities: 1827-2013. Drug Discov. Today 2014, 19, 1033–1039. [PubMed: 24680947]

(23). Yang Y; Hu X-Q; Li Q-S; Zhang X-X; Ruan B-F; Xu J; Liao C Metalloprotein Inhibitors for the Treatment of Human Diseases. Curr. Top. Med. Chem 2016, 16, 384–396. [PubMed: 26268345]

(24). Britten CD; Rowinsky EK; Soignet S; Patnaik A; Yao SL; Deutsch P; Lee Y; Lobell RB; Mazina KE; McCreery H; Pezzuli S; Spriggs D A Phase I and Pharmacological Study of the Farnesyl Protein Transferase Inhibitor L-778,123 in Patients with Solid Malignancies. Clin. Cancer Res 2001, 7, 3894–3903. [PubMed: 11751480]

(25). Sebti SM; Hamilton AD Farnesyltransferase and Geranylgeranyltransferase I Inhibitors and Cancer Therapy: Lessons from Mechanism and Bench-to-Bedside Translational Studies. Oncogene 2000, 19, 6584–6593. [PubMed: 11426643]

(26). Jones RA; Katritzky AR N-Oxides and Related Compounds .17. The Tautomerism of Mercapto-Pyridine and Acylamino-Pyridine 1-Oxides. J. Chem. Soc 1960, 2937–2942.

(27). Turley PA; Fenn RJ; Ritter JC Pyrithiones as Antifoulants: Environmental Chemistry and Preliminary Risk Assessment. Biofouling 2000, 15, 175–182. [PubMed: 22115302]

(28). Pearson RG Hard and Soft Acids and Bases. J. Am. Chem. Soc 1963, 85, 3533–3539.

(29). Pearson RG Hard and Soft Acids and Bases HSAB.1. Fundamental Principles. J. Chem. Educ 1968, 45, 581–587.

(30). Martin DP; Cohen SM Nucleophile Recognition as an Alternative Inhibition Mode for Benzoic Acid Based Carbonic Anhydrase Inhibitors. Chem. Commun 2012, 48, 5259–5261.

(31). Credille CV; Chen Y; Cohen SM Fragment-Based Identification of Influenza Endonuclease Inhibitors. J. Med. Chem 2016, 59, 6444–6454. [PubMed: 27291165]

(32). Schonherr D; Wollatz U; Haznar-Garbacz D; Hanke U; Box KJ; Taylor R; Ruiz R; Beato S; Becker D; Weitschies W Characterisation of Selected Active Agents Regarding pK(a) Values, Solubility Concentrations and pH Profiles by SiriusT3. Eur. J. Pharm. Biopharm 2015, 92, 155–170. [PubMed: 25758123]

(33). Slater B; Mccormack A; Avdeef A; Comer JEA pH-Metric Log P .4. Comparison of Partition-Coefficients Determined by HPLC and Potentiometric Methods to Literature Values. J. Pharm. Sci 1994, 83, 1280–1283. [PubMed: 7830244]

(34). Lipinski CA; Lombardo F; Dominy BW; Feeney PJ Experimental and computational approaches to estimate solubility and permeability in drug discovery and development settings. Adv. Drug Deliver. Rev 2001, 46, 3–26.

(35). Veber DF; Johnson SR; Cheng HY; Smith BR; Ward KW; Kopple KD Molecular Properties that Influence the Oral Bioavailability of Drug Candidates. J. Med. Chem 2002, 45, 2615–2623. [PubMed: 12036371]

(36). Clark DE; Pickett SD Computational methods for the prediction of ‘drug-likeness’. Drug Discov. Today 2000, 5, 49–58.

(37). Congreve M; Carr R; Murray C; Jhoti H A Rule of Three for Fragment-Based Lead Discovery? Drug Discov. Today 2003, 8, 876–877.

(38). Lassalas P; Gay B; Lasfargeas C; James MJ; Tran V; Vijayendran KG; Brunden KR; Kozlowski MC; Thomas CJ; Smith AB; Huryn DM; Ballatore C Structure Property Relationships of Carboxylic Acid Isosteres. J. Med. Chem 2016, 59, 3183–3203. [PubMed: 26967507]

(39). Hughes JD; Blagg J; Price DA; Bailey S; DeCrescenzo GA; Devraj RV; Ellsworth E; Fobian YM; Gibbs ME; Gilles RW; Greene N; Huang E; Krieger-Burke T; Loesel J; Wager T; Whiteley L;

Zhang Y Physiochemical drug properties associated with in vivo toxicological outcomes. Bioorg. Med. Chem. Lett 2008, 18, 4872–4875. [PubMed: 18691886]

(40). Puerta DT; Cohen SM Examination of Novel Zinc-Binding Groups for Use in Matrix Metalloproteinase Inhibitors. Inorg. Chem 2003, 42, 3423–3430. [PubMed: 12767177]

(41). Martin DP; Blachly PG; McCammon JA; Cohen SM Exploring the Influence of the Protein Environment on Metal-Binding Pharmacophores. J. Med. Chem 2014, 57, 7126–7135. [PubMed: 25116076]

(42). Rotondo CM; Wright GD Inhibitors of Metallo-Beta-Lactamases. Curr. Opin. Microbiol 2017, 39, 96–105. [PubMed: 29154026]

(43). Nordmann P; Poirel L; Walsh TR; Livermore DM The Emerging NDM Carbapenemases. Trends Microbiol. 2011, 19, 588–595. [PubMed: 22078325]

(44). Kim Y; Cunningham MA; Mire J; Tesar C; Sacchettini J; Joachimiak A NDM-1, the Ultimate Promiscuous Enzyme: Substrate Recognition and Catalytic Mechanism. FASEB J. 2013, 27, 1917–1927. [PubMed: 23363572]

(45). Thomas PW; Zheng M; Wu SS; Guo H; Liu DL; Xu DG; Fast W Characterization of Purified New Delhi Metallo-beta-lactamase-1. Biochemistry 2011, 50, 10102–10113. [PubMed: 22029287]

(46). Yuan P; Bartlam M; Lou Z; Chen S; Zhou J; He X; Lv Z; Ge R; Li X; Deng T; Fodor E; Rao Z; Liu Y Crystal Structure of an Avian Influenza Polymerase PA(N) Reveals an Endonuclease Active Site. Nature 2009, 458, 909–913. [PubMed: 19194458]

(47). Crepin T; Dias A; Palencia A; Swale C; Cusack S; Ruigrok RWH Mutational and Metal Binding Analysis of the Endonuclease Domain of the Influenza Virus Polymerase PA Subunit. J. Virol 2010, 84, 9096–9104. [PubMed: 20592097]

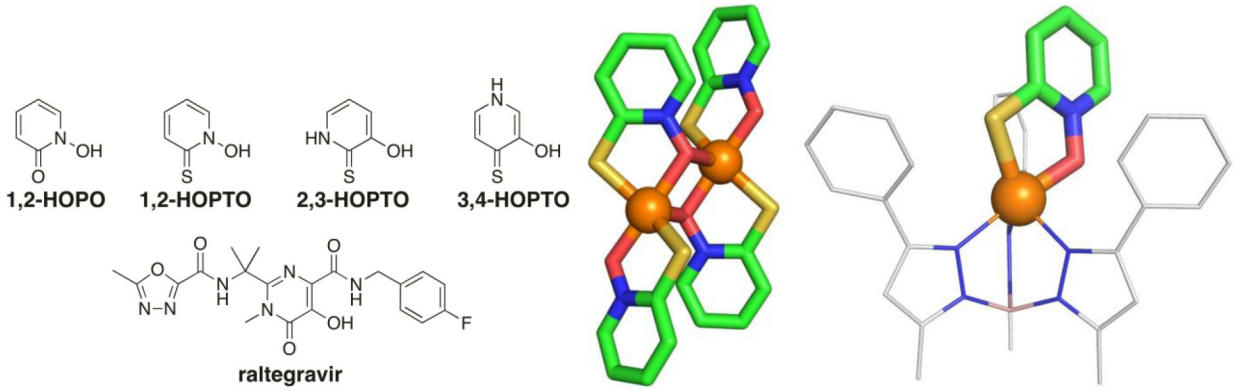

Figure 1.

The three HOPTO isomers, as well as a few examples of compounds containing HOPTO-like core scaffolds. The typical mode of HOPTO metal coordination is exemplified by the structures of $Zn(1,2\text{-HOPTO})_2$ (*middle*, CCDC: OXPZND) and [($Tp^{Ph,Me}$)Zn(1,2-HOPTO)] complex (*right*, CCDC: TADXUS). Structures are colored by atom type: boron = pink, carbon = green or gray, nitrogen = blue, oxygen = red, sulfur = gold, and zinc = orange (spheres).

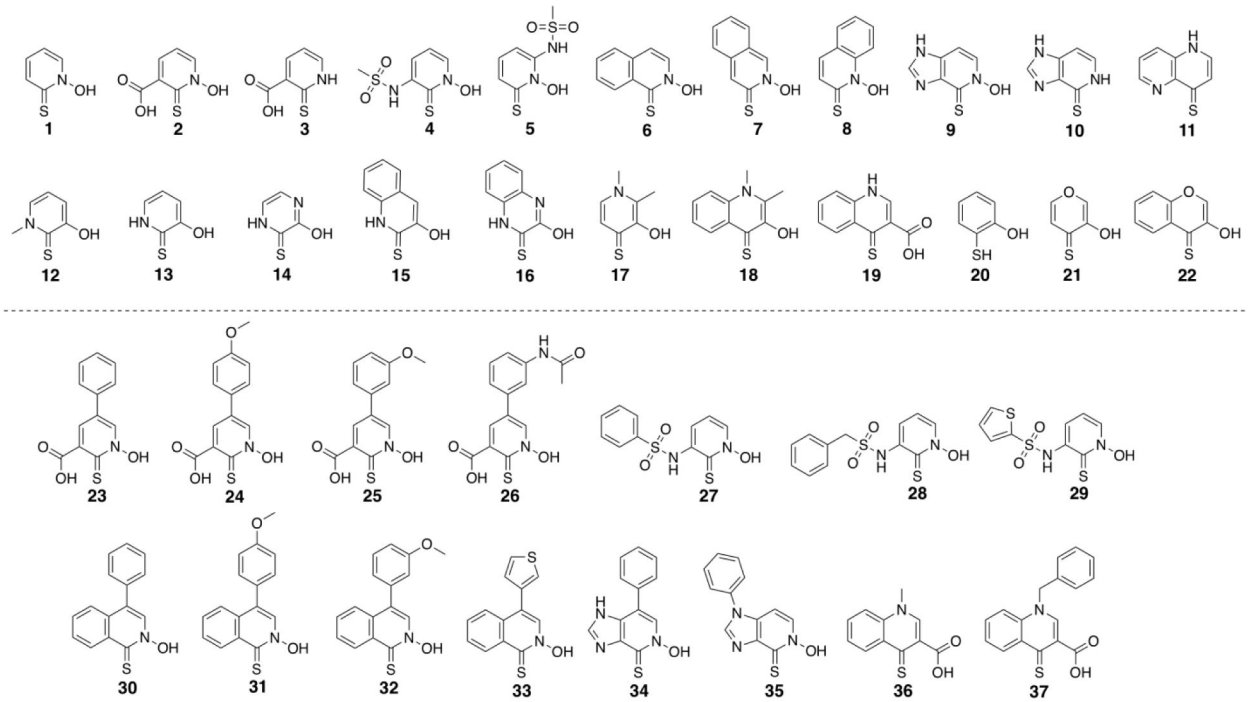

Figure 2.

Top: Assembled library of 22 HOPTO isostere compounds. *Bottom:* HOPTO isostere derivatives demonstrating the potential for additional functionalization.

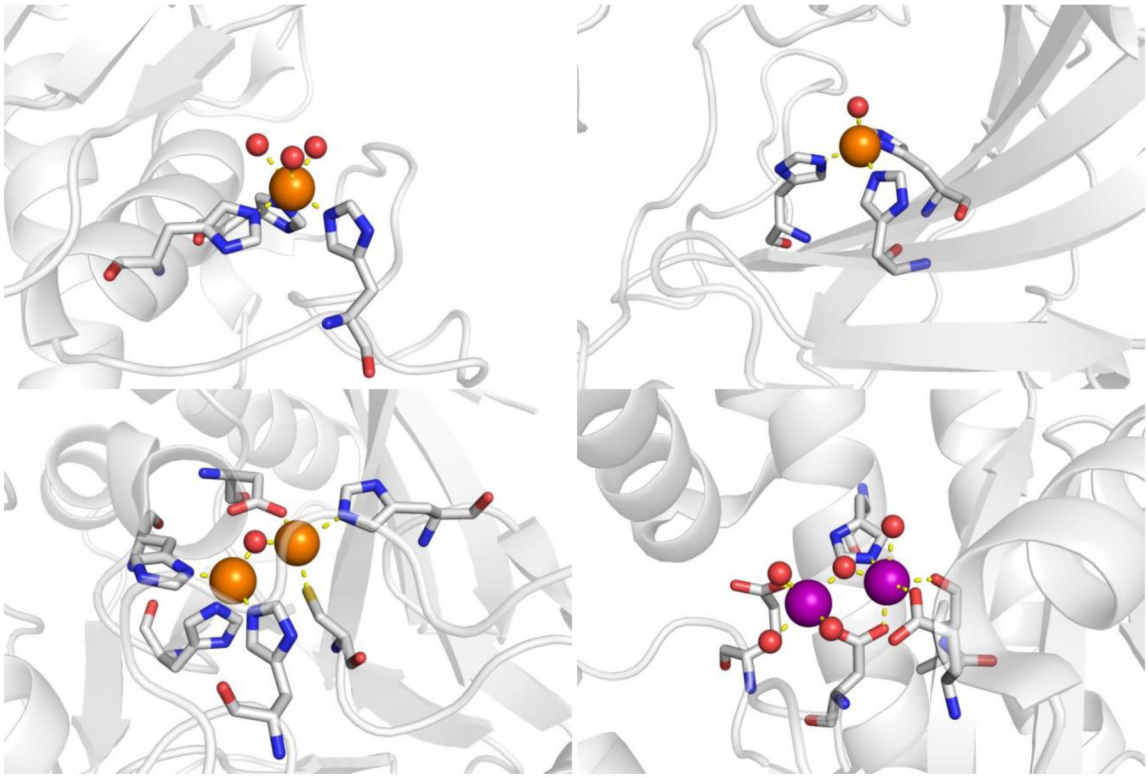

Figure 3.

Structures of metalloenzyme active sites used in this study. Metalloenzymes are shown as ribbons with coordinating residues shown in detail. Zn^{2+} is colored in orange spheres with Mn^{2+}/Mg^{2+} in purple, and coordination bonds are displayed as yellow dashes. *Upper left*: MMP-12 (2OXU). *Upper right*: hCAII (1CA2). *Bottom left*: NDM-1 (3SPU). *Bottom right*: influenza endonuclease (5DES).

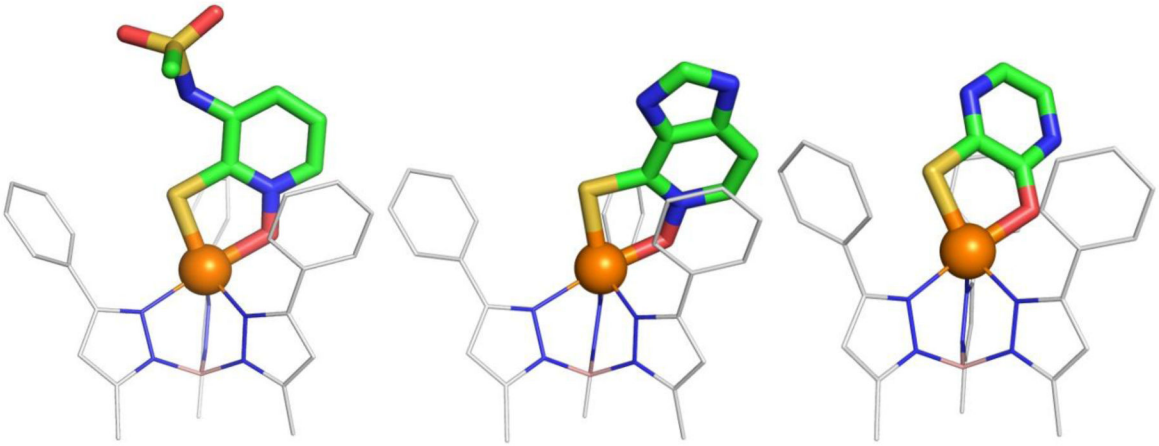

Figure 4.
The [(Tp^{Ph,Me})Zn(MBI)] complexes of compounds **4**, **9**, and **14**.

Table 1.

Summary of the properties used to assess the druglikeness of small molecules, as applied to both fully elaborated leads and fragments. The calculated PK values for each member of the HOPTO library is displayed below.

Compound	PSA (Å^2)	ClogP	ClogD$_{7.0}$	ClogS$_{7.0}$	H-Bond Donors	H-Bond Acceptors	Rotatable Bonds
Rule-of-Five	≤140 Å^2	≤5	≤5	≤−4	≤5	≤10	≤5
Rule-of-Three	≤ 60 Å^2	≤3	≤3	≤−4	≤3	≤3	≤3
1	55.56	0.91	0.90	−1.33	1	2	0
2	92.86	0.42	−2.44	0.49	2	4	1
3	81.42	0.63	−2.20	0.00	2	3	1
4	110.11	−0.38	−0.70	−1.24	2	4	2
5	110.11	−0.52	−0.32	−1.80	2	4	2
6	55.56	2.26	2.21	−3.29	1	2	0
7	55.56	0.99	1.06	−3.26	1	2	0
8	55.56	1.94	2.12	−3.18	1	2	0
9	84.24	0.13	0.33	−1.84	2	3	0
10	72.80	0.34	0.38	−2.85	2	2	0
11	57.01	1.40	1.36	−2.30	1	2	0
12	55.56	1.29	0.88	−1.11	1	2	0
13	64.35	1.04	0.66	−1.92	2	2	0
14	76.71	1.20	0.31	−1.15	2	3	0
15	64.35	2.54	2.22	−3.72	2	2	0
16	76.71	2.48	0.45	−0.78	2	3	0
17	55.56	1.73	1.50	−0.75	1	2	0
18	55.56	2.42	2.63	−2.55	1	2	0
19	81.42	1.82	1.07	−3.01	2	3	1
20	59.03	1.85	0.86	−0.56	1	1	0
21	61.55	1.63	1.23	−1.33	1	2	0
22	61.55	2.40	2.31	−3.15	1	2	0

Table 2.

Percent inhibition at 200 μM of the HOPTO isostere library against various metalloenzymes (enzyme concentrations and experimental details can be found in the Experimental section and SI). Percent inhibition is colored as a heat map with compounds that have no activity in yellow, and gradually moves towards compounds displaying complete inhibition in red.

Compound	MMP-12	hCAII	NDM-1	PA_N
1	11	13	69	43
2	40	0	77	70
3	34	0	0	10
4	99	3	100	73
5	94	10	96	93
6	98	88	100	33
7	13	41	5	98
8	23	29	8	44
9	28	9	93	42
10	56	5	0	16
11	96	9	100	30
12	53	4	40	40
13	40	10	83	40
14	42	0	12	41
15	44	23	54	24
16	50	24	41	3
17	94	11	98	0
18	44	0	38	37
19	53	2	63	32
20	14	22	19	0
21	66	19	93	100
22	35	47	79	90